Dielectron Widths of the $\Upsilon(1S, 2S, 3S)$ Resonances

J. L. Rosner,[1] N. E. Adam,[2] J. P. Alexander,[2] K. Berkelman,[2] D. G. Cassel,[2] J. E. Duboscq,[2] K. M. Ecklund,[2] R. Ehrlich,[2] L. Fields,[2] R. S. Galik,[2] L. Gibbons,[2] R. Gray,[2] S. W. Gray,[2] D. L. Hartill,[2] B. K. Heltsley,[2] D. Hertz,[2] C. D. Jones,[2] J. Kandaswamy,[2] D. L. Kreinick,[2] V. E. Kuznetsov,[2] H. Mahlke-Krüger,[2] T. O. Meyer,[2] P. U. E. Onyisi,[2] J. R. Patterson,[2] D. Peterson,[2] E. A. Phillips,[2] J. Pivarski,[2] D. Riley,[2] A. Ryd,[2] A. J. Sadoff,[2] H. Schwarthoff,[2] X. Shi,[2] S. Stroiney,[2] W. M. Sun,[2] T. Wilksen,[2] M. Weinberger,[2] S. B. Athar,[3] P. Avery,[3] L. Breva-Newell,[3] R. Patel,[3] V. Potlia,[3] H. Stoeck,[3] J. Yelton,[3] P. Rubin,[4] C. Cawlfield,[5] B. I. Eisenstein,[5] I. Karliner,[5] D. Kim,[5] N. Lowrey,[5] P. Naik,[5] C. Sedlack,[5] M. Selen,[5] E. J. White,[5] J. Wiss,[5] M. R. Shepherd,[6] D. Besson,[7] T. K. Pedlar,[8] D. Cronin-Hennessy,[9] K. Y. Gao,[9] D. T. Gong,[9] J. Hietala,[9] Y. Kubota,[9] T. Klein,[9] B. W. Lang,[9] R. Poling,[9] A. W. Scott,[9] A. Smith,[9] S. Dobbs,[10] Z. Metreveli,[10] K. K. Seth,[10] A. Tomaradze,[10] P. Zweber,[10] J. Ernst,[11] K. Arms,[12] H. Severini,[13] S. A. Dytman,[14] W. Love,[14] S. Mehrabyan,[14] V. Savinov,[14] O. Aquines,[15] Z. Li,[15] A. Lopez,[15] H. Mendez,[15] J. Ramirez,[15] G. S. Huang,[16] D. H. Miller,[16] V. Pavlunin,[16] B. Sanghi,[16] I. P. J. Shipsey,[16] B. Xin,[16] G. S. Adams,[17] M. Anderson,[17] J. P. Cummings,[17] I. Danko,[17] J. Napolitano,[17] Q. He,[18] J. Insler,[18] H. Muramatsu,[18] C. S. Park,[18] E. H. Thorndike,[18] T. E. Coan,[19] Y. S. Gao,[19] F. Liu,[19] R. Stroynowski,[19] M. Artuso,[20] S. Blusk,[20] J. Butt,[20] J. Li,[20] N. Menaa,[20] R. Mountain,[20] S. Nisar,[20] K. Randrianarivony,[20] R. Redjimi,[20] R. Sia,[20] T. Skwarnicki,[20] S. Stone,[20] J. C. Wang,[20] K. Zhang,[20] S. E. Csorna,[21] G. Bonvicini,[22] D. Cinabro,[22] M. Dubrovin,[22] A. Lincoln,[22] D. M. Asner,[23] K. W. Edwards,[23] R. A. Briere,[24] J. Chen,[24] T. Ferguson,[24] G. Tatishvili,[24] H. Vogel,[24] and M. E. Watkins[24]

(CLEO Collaboration)

[1]*Enrico Fermi Institute, University of Chicago, Chicago, Illinois 60637, USA*
[2]*Cornell University, Ithaca, New York 14853, USA*
[3]*University of Florida, Gainesville, Florida 32611, USA*
[4]*George Mason University, Fairfax, Virginia 22030, USA*
[5]*University of Illinois, Urbana-Champaign, Illinois 61801, USA*
[6]*Indiana University, Bloomington, Indiana 47405, USA*
[7]*University of Kansas, Lawrence, Kansas 66045, USA*
[8]*Luther College, Decorah, Iowa 52101, USA*
[9]*University of Minnesota, Minneapolis, Minnesota 55455, USA*
[10]*Northwestern University, Evanston, Illinois 60208, USA*
[11]*State University of New York at Albany, Albany, New York 12222, USA*
[12]*Ohio State University, Columbus, Ohio 43210, USA*
[13]*University of Oklahoma, Norman, Oklahoma 73019, USA*
[14]*University of Pittsburgh, Pittsburgh, Pennsylvania 15260, USA*
[15]*University of Puerto Rico, Mayaguez, Puerto Rico 00681*
[16]*Purdue University, West Lafayette, Indiana 47907, USA*
[17]*Rensselaer Polytechnic Institute, Troy, New York 12180, USA*
[18]*University of Rochester, Rochester, New York 14627, USA*
[19]*Southern Methodist University, Dallas, Texas 75275, USA*
[20]*Syracuse University, Syracuse, New York 13244, USA*
[21]*Vanderbilt University, Nashville, Tennessee 37235, USA*
[22]*Wayne State University, Detroit, Michigan 48202, USA*
[23]*Carleton University, Ottawa, Ontario, Canada K1S 5B6*
[24]*Carnegie Mellon University, Pittsburgh, Pennsylvania 15213, USA*
(Received 21 December 2005; published 9 March 2006)

We determine the dielectron widths of the $\Upsilon(1S)$, $\Upsilon(2S)$, and $\Upsilon(3S)$ resonances with better than 2% precision by integrating the cross section of $e^+e^- \to \Upsilon$ over the e^+e^- center-of-mass energy. Using e^+e^- energy scans of the Υ resonances at the Cornell Electron Storage Ring and measuring Υ production with the CLEO detector, we find dielectron widths of $1.252 \pm 0.004(\sigma_{\text{stat}}) \pm 0.019(\sigma_{\text{syst}})$ keV, $0.581 \pm 0.004 \pm 0.009$ keV, and $0.413 \pm 0.004 \pm 0.006$ keV for the $\Upsilon(1S)$, $\Upsilon(2S)$, and $\Upsilon(3S)$, respectively.

DOI: 10.1103/PhysRevLett.96.092003 PACS numbers: 14.40.Nd, 12.20.Fv, 13.25.Gv

The widths of the Υ mesons, $b\bar{b}$ bound states discovered in 1977 [1], are related to the quark-antiquark spatial wave function at the origin [2]. These widths provide a testing ground for QCD lattice gauge theory calculations [3]. Improvements in the lattice calculations, such as avoidance of the quenched approximation [4], provide an incentive for more accurate experimental tests. The dielectron widths (Γ_{ee}) of the $\Upsilon(1S)$, $\Upsilon(2S)$, and $\Upsilon(3S)$ have previously been measured with precisions of 2.2%, 4.2%, and 9.4%, respectively [5]. Validation of the lattice calculations at an accuracy of a few percent will increase confidence in similar calculations used to extract important weak-interaction parameters from data. In particular, Γ_{ee} and f_D [6] provide complementary tests of the calculation of f_B, which is used to determine the Cabibbo-Kobayashi-Maskawa matrix element V_{td}.

Our measurement of Γ_{ee} follows the method of [5]: we integrate the production cross section of Υ over incident e^+e^- energies. If we ignore initial-state radiation for clarity, the partial width is given by

$$\Gamma_{ee} = \frac{M_\Upsilon^2}{6\pi^2} \int \sigma(e^+e^- \to \Upsilon) dE. \quad (1)$$

We also determine the Υ full widths using $\Gamma = \Gamma_{ee}/\mathcal{B}_{\ell\ell}$, where $\mathcal{B}_{\ell\ell}$ is the Υ branching fraction to a pair of leptons.

The Cornell Electron Storage Ring (CESR), an e^+e^- collider, scanned center-of-mass energies in the vicinity of the $\Upsilon(1S)$, $\Upsilon(2S)$, and $\Upsilon(3S)$, and the CLEO III detector collected the Υ decay products to determine the cross section at each energy. A fit to this resonance line shape yields $\int \sigma(e^+e^- \to \Upsilon) dE$. This fit includes the effects of initial-state radiation, beam energy spread, backgrounds, and interference between Υ and continuum decays. The eleven $\Upsilon(1S)$ scans, six $\Upsilon(2S)$ scans, and seven $\Upsilon(3S)$ scans have integrated luminosities of 0.27, 0.08, and 0.22 fb^{-1}, respectively, with 0.19, 0.41, and 0.14 fb^{-1} of data below each peak to constrain backgrounds.

The CLEO III detector is a nearly 4π tracking volume surrounded by a CsI crystal calorimeter [7,8]. Charged tracks are reconstructed in a 47-layer wire drift chamber and 4-layer silicon strip detector, and their momenta are inferred from their radii of curvature in a 1.5 T magnetic field. The calorimeter forms a cylindrical barrel around the tracking volume, reaching angles θ with respect to the beam axis of $|\cos\theta| < 0.85$, with end caps extending this range to $|\cos\theta| < 0.98$. Electron showers have a resolution of 75 MeV at 5 GeV (the beam energy).

The Υ mesons are produced nearly at rest and decay into leptonic final states e^+e^-, $\mu^+\mu^-$, or $\tau^+\tau^-$, or into hadrons via ggg, $gg\gamma$, or $q\bar{q}$ intermediate states. The $\Upsilon(2S)$ and $\Upsilon(3S)$ can also make transitions into other $b\bar{b}$ resonances such as $\chi_{bJ}(nP)$, $\Upsilon(1S)$, and $\Upsilon(2S)$. The leptonic decays together account for only about 7% of the decays of each resonance and are difficult to distinguish from background, so we select hadrons, fit the hadronic cross section, and report $\Gamma_{ee}\Gamma_{\rm had}/\Gamma_{\rm tot}$. We then correct for the missing leptonic modes to report Γ_{ee}, assuming $\mathcal{B}_{ee} = \mathcal{B}_{\mu\mu} = \mathcal{B}_{\tau\tau}$ and obtaining the well-measured $\mathcal{B}_{\mu\mu}$ from [9]. (The τ mass shifts $\mathcal{B}_{\tau\tau}$ below the $\mathcal{B}_{ee}$ or $\mathcal{B}_{\mu\mu}$ expectation by only 0.05% at these energies.) Thus, $\Gamma_{ee} = (\Gamma_{ee}\Gamma_{\rm had}/\Gamma_{\rm tot})/(1 - 3\mathcal{B}_{\mu\mu})$.

Bhabha scattering ($e^+e^- \to e^+e^-$) is our largest potential background. We suppress these events by requiring the greatest track momentum ($P_{\rm max}$) to be less than 80% of the beam energy, shown in Fig. 1(a), which reduces the Bhabha background to approximately the same magnitude as the hadronic continuum ($e^+e^- \to q\bar{q}$) background. Continuum annihilation processes such as these are accounted for by including a $1/s$ term in the line shape fit, where $s = E_{\rm CM}{}^2 = (2E_{\rm beam})^2$.

The contribution of two-photon events ($e^+e^- \to e^+e^-X$) grows with log$s$. We suppress these by requiring the total visible energy (energy sum of all charged tracks and neutral showers) to be more than 40% of the center-of-mass energy, shown in Fig. 1(b). The $\Upsilon(2S)$ and $\Upsilon(3S)$ additionally have backgrounds from radiative returns to each lower-energy resonance, with a cross section inversely proportional to the initial-state photon energy. We therefore add to the fit function a small log$s$ term (8% of continuum at 9 GeV) and $1/(\sqrt{s} - M_\Upsilon)$ terms for $\Upsilon(1S)$ and $\Upsilon(2S)$ (about 0.5% of continuum at the $\Upsilon(3S)$). Because the off-resonance data are only 20 MeV below each peak, the different functional forms affect the background estimation at the peak by less than 0.04%.

Cosmic rays and beam-gas interactions (collisions between a beam electron and a gas nucleus inside the beam pipe) are suppressed by requiring charged tracks to point toward the beam-beam intersection point. We reduce this to less than 1% of the continuum by demanding that at least one reconstructed track pass within 5 mm of the beam axis and the vertex reconstructed from all primary tracks be within 7.5 cm of the intersection point along the beam axis. We determine and subtract the remaining contamination at

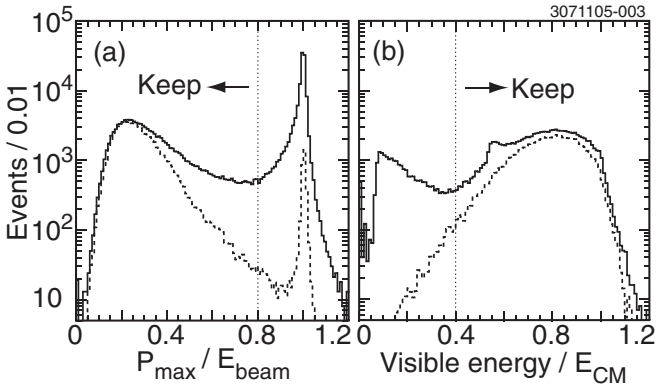

FIG. 1. Two of the distributions used to identify hadronic Υ decays. Solid histograms are data, dashed are simulated $\Upsilon(1S)$ decays, both with all hadronic selection criteria applied except the one shown. Dotted lines indicate selection thresholds.

each energy using special single-beam and no-beam data runs normalized using events with a solitary large impact parameter track (for cosmic rays) or vertices along the beam axis but far from the collision point (for beam gas). Individual backgrounds for the $\Upsilon(3S)$ are illustrated in Fig. 2.

While our hadronic selection criteria eliminate essentially all $\Upsilon \to e^+e^-$ and $\Upsilon \to \mu^+\mu^-$ decays, they accept 57% of $\Upsilon \to \tau^+\tau^-$, according to a GEANT-based Monte Carlo simulation [10] including final-state radiation [11]. We therefore add to the fit function an $\Upsilon \to \tau^+\tau^-$ background term, including interference with continuum $e^+e^- \to \tau^+\tau^-$, using the measured $\mathcal{B}_{\tau\tau}$ [12].

A small fraction of hadronic Υ decays fail our event selection criteria. Instead of estimating this inefficiency with the Monte Carlo simulation, which would introduce dependence on the decay model, hadronization model, and detector simulation, we use a data-based approach. We select $\Upsilon(2S) \to \pi^+\pi^-\Upsilon(1S)$ events to study $\Upsilon(1S)$ decays tagged by $\pi^+\pi^-$. If the $\pi^+\pi^-$ were sufficient to satisfy the trigger, the efficiency would be the ratio of $\Upsilon(1S)$ events satisfying our selection criteria (excluding the $\pi^+\pi^-$ tracks and showers) to all $\Upsilon(1S)$ events.

Although this procedure could be applied directly to the $\Upsilon(2S)$ sample, the loose two-track trigger involved is prescaled, and thus can only determine the hadronic efficiency to within 3% of itself. Instead, we use the two-track trigger to determine the efficiency of a nonprescaled but more restrictive hadronic trigger ($\epsilon_{\rm htrig}$), and then use the full statistics from the hadronic trigger to determine our selection efficiency once this trigger has been satisfied ($\epsilon_{\rm cuts}$). Our combined event selection and trigger efficiency is then the product of $\epsilon_{\rm htrig}$ and $\epsilon_{\rm cuts}$.

The mass of the system recoiling against the $\pi^+\pi^-$ candidates in the two-track trigger sample is shown in Fig. 3. After correcting for leptonic decays in the $\Upsilon(1S)$ sample, we find $\epsilon_{\rm htrig} = (99.59^{+0.29}_{-0.45})\%$ from the ratio of fit yields.

From $\Upsilon(2S) \to \pi^+\pi^-\Upsilon(1S)$ events that satisfy the hadronic trigger, we find $\epsilon_{\rm cuts} = (98.33 \pm 0.33)\%$. This has been corrected for leptonic decays, the boost of the $\Upsilon(1S)$, track and shower confusion from the $\pi^+\pi^-$, and the efficiency of the full set of triggers. Only the first correction is significant. Our event selection and trigger efficiency is therefore $(97.93^{+0.44}_{-0.56})\%$ for the sum of all nonleptonic $\Upsilon(1S)$ decays.

To find the $\Upsilon(2S)$ and $\Upsilon(3S)$ efficiencies, we correct the $\Upsilon(1S)$ efficiency for energy dependence and for transitions specific to these excited states, using simulations. Energy dependence is negligible; only transitions to lower Υ resonances which then decay to e^+e^- or $\mu^+\mu^-$ introduce a significant loss of efficiency. We measure the branching fractions of these decays to be $(1.58 \pm 0.16)\%$ and $(1.34 \pm 0.13)\%$, respectively, resulting in $\Upsilon(2S)$ and $\Upsilon(3S)$ efficiencies of $(96.18^{+0.44}_{-0.56} \pm 0.15)\%$ and $(96.41^{+0.44}_{-0.56} \pm 0.13)\%$. Both uncertainties are statistical, but the first is common to all three resonances.

We use Bhabha events to determine the relative luminosity of each scan point. We select the Bhabhas by requiring two or more central tracks with momenta between 50% and 110% of the beam energy, and a ratio of shower energy to track momentum consistent with e^+ and e^-. Contamination from $\Upsilon \to e^+e^-$ is 2%–5% and is readily calculated given $\mathcal{B}_{ee}$ once we have done our Υ line shape fit. Our subtraction includes energy-dependent interference between $\Upsilon \to e^+e^-$ and Bhabhas.

We determine the overall luminosity scale using the method of [13] from Bhabhas, $e^+e^- \to \mu^+\mu^-$, and $e^+e^- \to \gamma\gamma$, with the Babayaga event generator [14]. The systematic uncertainties from the three processes are 1.6%, 1.6%, and 1.8%, respectively, dominated by track finding and resonance interference for e^+e^- and $\mu^+\mu^-$, and by photon finding and angular resolution for $\gamma\gamma$. The three measurements give consistent results off resonance,

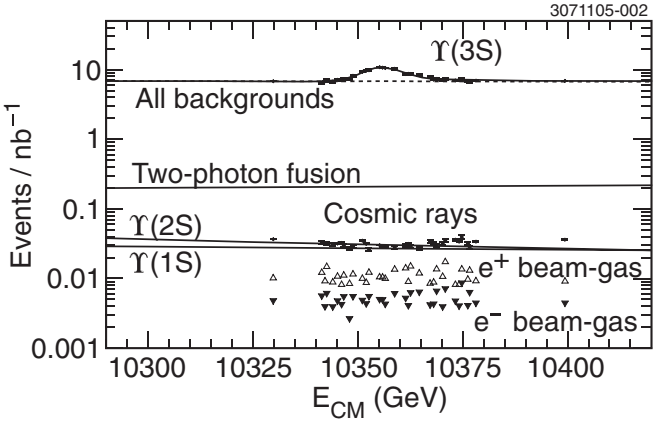

FIG. 2. The event yield as a function of center-of-mass energy in the region of the $\Upsilon(3S)$. The top points are data, with the fit superimposed, and the dashed curve represents the sum of all backgrounds. The lower points and lines show the individual non-$1/s$ background contributions.

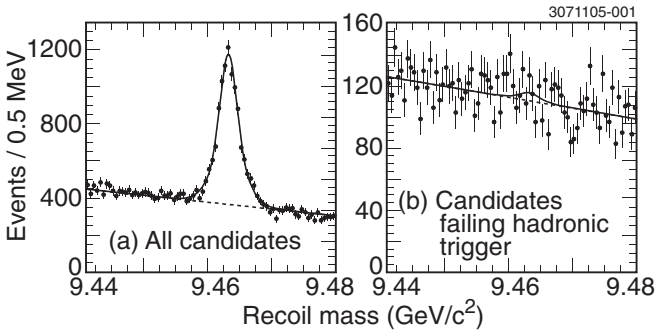

FIG. 3. Mass of the system recoiling against the $\pi^+\pi^-$ in $\Upsilon(2S) \to \pi^+\pi^-\Upsilon(1S)$ candidates satisfying the two-track trigger, for (a) all events, and (b) events that satisfy the hadronic trigger. The dashed curve represents backgrounds and the solid curve represents the sum of backgrounds and the recoiling $\Upsilon(1S)$ signal.

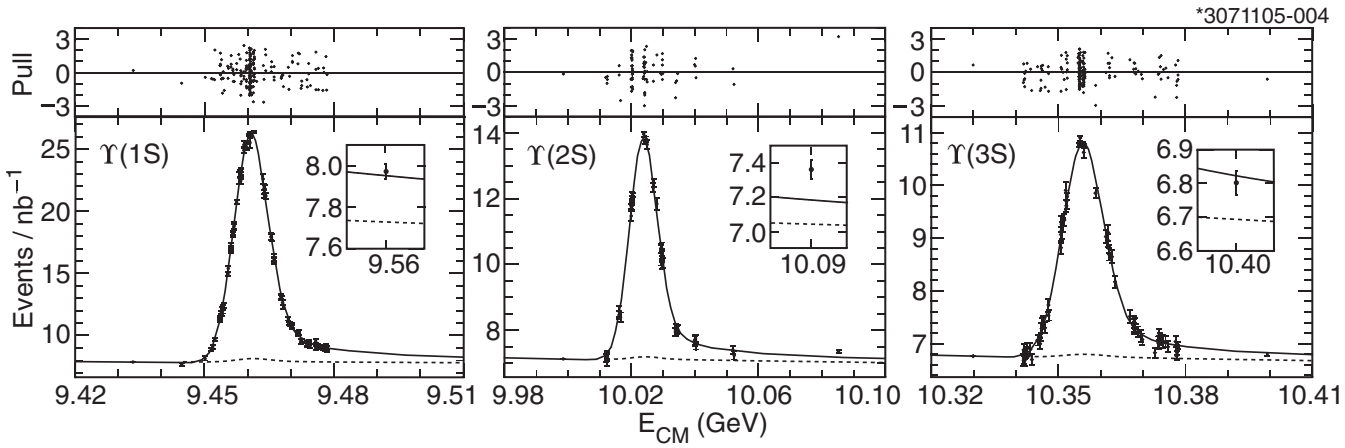

FIG. 4. The hadronic yield vs center-of-mass energy in the vicinity of the three Υ resonances. Points represent the data, corrected for fitted beam energy shifts between scans, the solid line is the fit, the dashed line is the sum of all backgrounds, and the insets show high-energy measurements. The pull of each point is shown above.

where Υ contamination is negligible. We use the weighted mean to determine the luminosity, and take the root mean square scatter of 1.3% as the systematic uncertainty.

Bhabha and $\gamma\gamma$ luminosities, normalized to the same value off resonance, deviate by $(0.8 \pm 0.2)\%$, $(0.3 \pm 0.4)\%$, and $(0.7 \pm 0.2)\%$ at the $\Upsilon(1S)$, $\Upsilon(2S)$, and $\Upsilon(3S)$ peaks. We correct each Γ_{ee} by half of its discrepancy and take half the discrepancy and its uncertainty in quadrature as a systematic uncertainty.

Accurate measurement of beam energies are also needed to determine Γ_{ee}. An NMR probe calibrates the field of the CESR dipole magnets and hence provides the beam energy, after corrections for rf shifts, steering and focusing magnets, and electrostatic electron-positron separators. To limit our sensitivity to drifts in this measurement, we limit scans to 48 hours and alternate measurements above and below the peak. By repeating a resonance cross section measurement at a point of high slope, we find that the beam energy calibration drifts by less than 0.04 MeV within a scan (at 68% confidence level), which implies a 0.2% uncertainty in Γ_{ee}.

The data for each resonance are separately fit to a function that consists of a threefold convolution of (a) a Breit-Wigner resonance including interference between $\Upsilon \to q\bar{q}$ and $e^+e^- \to q\bar{q}$ with zero phase difference at $\sqrt{s} \ll M_\Upsilon$, (b) an initial-state radiation distribution as given in Equation (28) of [15], and (c) the Gaussian spread in CESR beam energy of about 4 MeV, plus the background terms described above. The radiative corrections account for emission of real and virtual photons by the initial e^+e^-. We do not correct for vacuum polarization, which is absorbed into the definition of Γ_{ee}. The resulting Γ_{ee} therefore represents the Born diagram coupling of a pure e^+e^- state to the Υ. The fits are insensitive to the Breit-Wigner widths at the 0.1% level, so we fix these widths to the current world averages [5]. The value of $\Gamma_{ee}\Gamma_{\rm had}/\Gamma_{\rm tot}$ of each resonance is allowed to float, as is the continuum normalization, and, to remove sensitivity to beam energy shifts between scans, the peak energy of each scan. In addition, we fit for the beam energy spread of groups of scans with common CESR horizontal steerings, but allow shifts when the steerings change, since they can change the beam energy spread by 1%.

The fit results are plotted in Fig. 4. The fit function describes the data well, though it results in larger χ^2 values for the $\Upsilon(1S)$ and $\Upsilon(2S)$. The χ^2 per degree of freedom ($N_{\rm dof}$) for $\Upsilon(1S)$ is 240/187 (0.5% confidence level), for $\Upsilon(2S)$ is 107/66 (0.1% confidence level), and for $\Upsilon(3S)$ is 155/159 (59% confidence level). We see no obvious trends in pull (residual divided by uncertainty) versus energy or versus date, so we take the large χ^2 values as an indication that point-to-point uncertainties are underestimated, and add $\sigma_{\rm stat}\sqrt{\chi^2/N_{\rm dof} - 1}$ to the systematic uncertainty, if $\chi^2/N_{\rm dof} > 1$. This effectively multiplies the statistical un-

TABLE I. All uncertainties in Γ_{ee}. The correction for leptonic modes is made for Γ_{ee} but not $\Gamma_{ee}\Gamma_{\rm had}/\Gamma_{\rm tot}$. The uncertainties in hadronic efficiency and overall luminosity scale are common to all three resonances.

Contribution to Γ_{ee}	$\Upsilon(1S)$	$\Upsilon(2S)$	$\Upsilon(3S)$
Correction for leptonic modes	0.2%	0.2%	0.3%
Hadronic efficiency	0.5%	0.5%	0.5%
Xe^+e^-, $X\mu^+\mu^-$ correction	0	0.15%	0.13%
Overall luminosity scale	1.3%	1.3%	1.3%
Bhabha/$\gamma\gamma$ inconsistency	0.4%	0.4%	0.4%
Beam energy measurement drift	0.2%	0.2%	0.2%
Fit function shape	0.1%	0.1%	0.1%
χ^2 inconsistency	0.2%	0.6%	0
Total systematic uncertainty	1.5%	1.6%	1.5%
Statistical uncertainty	0.3%	0.7%	1.0%
Total	1.5%	1.8%	1.8%

TABLE II. The results of $\Gamma_{ee}\Gamma_{\rm had}/\Gamma_{\rm tot}$ for the three resonances, the dielectron widths Γ_{ee}, and their ratios. The first uncertainty is statistical and the second is systematic.

$\Gamma_{ee}\Gamma_{\rm had}/\Gamma_{\rm tot}(1S)$	$1.252 \pm 0.004 \pm 0.019$ keV
$\Gamma_{ee}\Gamma_{\rm had}/\Gamma_{\rm tot}(2S)$	$0.581 \pm 0.004 \pm 0.009$ keV
$\Gamma_{ee}\Gamma_{\rm had}/\Gamma_{\rm tot}(3S)$	$0.413 \pm 0.004 \pm 0.006$ keV
$\Gamma_{ee}(1S)$	$1.354 \pm 0.004 \pm 0.020$ keV
$\Gamma_{ee}(2S)$	$0.619 \pm 0.004 \pm 0.010$ keV
$\Gamma_{ee}(3S)$	$0.446 \pm 0.004 \pm 0.007$ keV
$\Gamma_{ee}(2S)/\Gamma_{ee}(1S)$	$0.457 \pm 0.004 \pm 0.004$
$\Gamma_{ee}(3S)/\Gamma_{ee}(1S)$	$0.329 \pm 0.003 \pm 0.003$
$\Gamma_{ee}(3S)/\Gamma_{ee}(2S)$	$0.720 \pm 0.009 \pm 0.007$

certainty ($\sigma_{\rm stat}$) by $\sqrt{\chi^2/N_{\rm dof}}$. All uncertainties are listed in Table I.

We assume that $e^+e^- \to q\bar{q}$ interferes only with the $q\bar{q}$ component of hadronic Υ decays. The $\Upsilon(1S)$ fit favors this interference scheme over the no-interference hypothesis by 3.7 standard deviations. It is also possible that $e^+e^- \to q\bar{q} \to$ hadrons interferes with $\Upsilon \to ggg \to$ hadrons. If so, full interference between all final states, all with a common phase difference near $\pm\pi/2$ ($\Upsilon \to ggg$ phase minus $\Upsilon \to q\bar{q}$ phase), would shift $\Gamma_{ee}\Gamma_{\rm had}/\Gamma_{\rm tot}$ by $\mp 5.4\%$, $\mp 3.8\%$, and $\mp 3.5\%$ for the $\Upsilon(1S)$, $\Upsilon(2S)$, and $\Upsilon(3S)$, respectively [16]. This is the most extreme case. Overlap of isospin and flavor states for these two processes suggest that this interference, if it occurs, affects $\Gamma_{ee}\Gamma_{\rm had}/\Gamma_{\rm tot}$ at no more than the $\sim 1\%$ level.

Our values of $\Gamma_{ee}\Gamma_{\rm had}/\Gamma_{\rm tot}$, listed in Table II, are consistent with, but more precise than, the PDG world averages [5] and our $\Upsilon(3S)$ measurement is substantially more precise. Also listed in the Table are the dielectron widths and ratios of these widths, in which common systematic uncertainties have been canceled. Assuming $\mathcal{B}_{ee} = \mathcal{B}_{\mu\mu}$ and using [9], we obtain new values of the Υ full widths: $54.4 \pm 0.2(\sigma_{\rm stat}) \pm 0.8(\sigma_{\rm syst}) \pm 1.6(\sigma_{\mathcal{B}_{\mu\mu}})$ keV for the $\Upsilon(1S)$, $30.5 \pm 0.2 \pm 0.5 \pm 1.3$ keV for the $\Upsilon(2S)$, and $18.6 \pm 0.2 \pm 0.3 \pm 0.9$ keV for the $\Upsilon(3S)$.

We gratefully acknowledge the effort of the CESR staff in providing us with excellent luminosity and running conditions. This work was supported by the A. P. Sloan Foundation, the National Science Foundation, and the U.S. Department of Energy.

[1] S. W. Herb *et al.*, Phys. Rev. Lett. **39**, 252 (1977).
[2] R. Van Royen and V. F. Weisskopf, Nuovo Cimento A **50**, 617 (1967); **51**, 583(E) (1967).
[3] A. Gray, I. Allison, C. T. H. Davies, E. Gulez, G. P. Lepage, J. Shigemitsu, and M. Wingate, Phys. Rev. D **72**, 094507 (2005).
[4] C. T. H. Davies *et al.* (HPQCD Collaboration), Phys. Rev. Lett. **92**, 022001 (2004).
[5] S. Eidelman *et al.* (Particle Data Group), Phys. Lett. B **592**, 1 (2004).
[6] M. Artuso *et al.* (CLEO Collaboration), Phys. Rev. Lett. **95**, 251801 (2005).
[7] G. Viehhauser, Nucl. Instrum. Methods Phys. Res., Sect. A **462**, 146 (2001).
[8] D. Peterson *et al.*, Nucl. Instrum. Methods Phys. Res., Sect. A **478**, 142 (2002).
[9] G. S. Adams *et al.* (CLEO Collaboration), Phys. Rev. Lett. **94**, 012001 (2005).
[10] R. Brun *et al.*, GEANT 3.21, CERN Program Library Long Writeup Report No. W5013, 1993 (unpublished).
[11] E. Barberio and Z. Wąs, Comput. Phys. Commun. **79**, 291 (1994).
[12] J. E. Duboscq (CLEO Collaboration), hep-ex/0601036.
[13] G. D. Crawford *et al.* (CLEO Collaboration), Nucl. Instrum. Methods Phys. Res., Sect. A **345**, 429 (1994).
[14] C. M. Carloni Calame *et al.*, Nucl. Phys. Proc. Suppl. **131**, 48 (2004).
[15] E. A. Kuraev and V. S. Fadin, Yad. Fiz. **41**, 733 (1985) [Sov. J. Nucl. Phys. **41**, 466 (1985)].
[16] J. Pivarski, Ph.D. thesis, Cornell University (unpublished).